Supplementary Material Cover Sheet

Biosurfactant-mediated the mobility of graphene oxide nanoparticles in saturated porous media

Jiuyan Chen [1, 2], Qiang Zhang [3], Yuwei Zhu [2], Yanxiang Li [4], Weifeng Chen [5], Taotao Lu [1, *], and Zhichong Qi [2, **]

[1] College of Hydraulic Science and Engineering, Yangzhou University, Yangzhou, 225009, China

[2] Henan Joint International Research Laboratory of Environmental Pollution Control Materials, College of Chemistry and Chemical Engineering, Henan University, Kaifeng 475004, China

[3] Ecology institute of the Shandong academy of sciences, Qilu University of Technology (Shandong Academy of Sciences), Jinan 250353, China

[4] The Testing Center of Shandong Bureau, China Metallurgical Geology Bureau, Jinan 250014, China

[5] Key Laboratory for Humid Subtropical Eco-geographical Processes of the Ministry of Education/ Fujian Provincial Key Laboratory for Plant Eco-physiology/ School of Geographical Sciences, Fujian normal university, Fuzhou, Fujian 350007, China

Manuscript prepared for *Environmental Science-Processes & Impacts*

[*]Corresponding author: Taotao Lu (Taotao.Lu@yzu.edu.cn);

[**]Corresponding author: Zhichong Qi (qizhichong1984@163.com).

Number of pages: 30

Number of tables: 5

Number of figures: 13

S1. Preparation of goethite-coated sand

In order to produce heterogeneous porous media surfaces that reflect conditions commonly encountered in the subsurface environment. Before use, the sand was cleaned to remove metal oxides and organics on the grain surface using the method of Xia et al.[S1]

The procedure which coated with goethite was similar to that reported Stahl and James.[S2] In brief, goethite-coated sand was precipitated onto 500 g of quartz sand by adding 87.5 mL of 0.17 M Fe $(NO_3)_3$ and 90.0 mL of 0.52 M NaOH in an evaporating dish. The mixture was placed in a drying oven at 105 ^oC for 72 h. The mixture was stirred periodically to prevent crusting of the salts on the surface. After coating the quartz sand with goethite, the sand was washed in 1.0 mM HCl and 1.0 mM NaOH to remove weakly absorbed iron on the sand surface.

S2. Determine of the ζ-potential of the porous media

The zeta potential of sand grains (including the uncoated and iron oxide-coated sand) was measured by using a Zeta-Plus potential analyzer (Zetasizer nano ZS90, Malvern Instruments, UK) at room temperature (25°C) according to the method described in previous studies.[S3,S4] It should be noted that, because the sand grains were too large for direct measurement by the zeta potential analyzer, a few sand grains were crushed into fine powders and then mixed with the appropriate chemistry solution (see Table 1) in an ultrasonic bath for 30 min. Then, the mixture was formed a sufficiently stable suspension that could be used for zeta potential measurement.

S3. Procedures used to obtain retention profiles of GO in columns

To obtain the retention profiles of GO in the columns at the end of the transport experiments, the sand columns were dissected into 10 layers of 1-cm segments and subsequently re-entrained to DI water,[S5] then agitating for 3 h on an oscillating shaker (KS 260 Basic, IKA). Then, the vials were centrifuged at 3,000 rpm for 20 min, and the supernatants were withdrawn to measure the concentrations of GO. In the absence of saponin, GO concentrations were measured using the UV absorbance at 230 nm (Purkinje General Instrument Co., Ltd., Beijing, China). In the presence of saponin, the concentrations of GO were determined according to the method described by Chen et al.[S6]

S4. Adsorption of saponin onto sand and goethite-coated sand.

Adsorption experiments were also conducted to determine the adsorbed amount of saponin onto sand and goethite-coated sand under different solution chemistry conditions. The initial concentrations of saponin in the 20-mL amber glass vial were 3–10 mg/L; and the initial mass of sand was 5 g. The vials were mixed the vials were left on an orbital shaker operated at room temperature for 12 h. The liquid and solid phases were separated by centrifugation at 5000 rpm for 30 min, and then the supernatants were filtered through 0.45 μm filtering membrane. Aqueous bio-surfactant concentrations in the supernatants were quantified using the UV absorbance at 263 nm (Purkinje General Instrument Co., Ltd., Beijing, China).[S7]

S5. Calculation of XDLVO interaction energy

Given that GO is a carbon sheet with the identical length of carbon bond, a cuboid-plate configuration was used to calculate the interaction energy between GO and quartz sand or goethite-coated sand (as shown in the following figure) [S8].

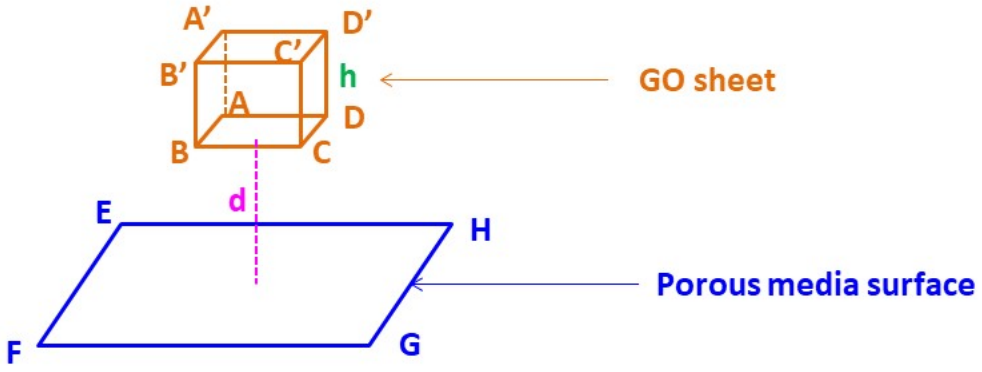

The total interaction energy (V_{TOT}) between GO and porous media using the cuboid-plate configuration was determined as follows:

$$V_{TOT} = V^{TOT}_{EFGH-ABCD}(d) - V^{TOT}_{EFGH-A'B'C'D'}(d+h) \quad \text{(S1)}$$

where d is the separation distance between a surface element on the GO bottom surface and the collector surface; and h is the thickness of the GO. Note that the thickness of GO under different solution chemistry conditions were obtained based on our previous studies. [S9–S11].

According to the extended Derjaguin-Landau-Verwey-Overbeek (XDLVO) theory, the total interaction energy between particle and collector (V_{TOT}) can be defined as the sum of four interactions, the attractive van der Waals interaction energy (V_{VDW}), the repulsive electrostatic double layer interaction (V_{EDL}), Born repulsive interaction energy (V_{BR}), and hydration repulsive interaction energy (V_{HR}):[S12]

$$V_{TOT} = V_{VDW} + V_{EDL} + V_{BR} + V_{HR} \quad \text{(S2)}$$

The van der Waals interaction is calculated using the Hamaker approach and Gregory's formulation:[S13]

$$V_{VDW} = -\frac{Aa_p}{6h\left(1+\frac{14h}{\lambda}\right)} \quad \text{(S3)}$$

where a_p is the radius of GO nanoparticles (the data were obtained based on direct TEM evidence in Table S3), λ is the characteristic wavelength of GO nanoparticles (λ = 100 nm), and A is the Hamaker constant. For GO nanoparticles and sand/goethite-coated sand interaction, The Hamaker constant of GO nanoparticles -water-sand system can be calculated by following equation:[S14]

$$A_{132} = \left(\sqrt{A_{11}} - \sqrt{A_{33}}\right)\left(\sqrt{A_{22}} - \sqrt{A_{33}}\right) \quad \text{(S4)}$$

where A_{132} is the Hamaker constant for the material 1 (GO nanoparticles) interaction with the material 2 (collector) through the material 3 (water), A_{11} is the Hamaker constant of GO nanoparticles, which is 6.34×10^{-20} J.[S15] A_{22} is the Hamaker constant of the collector surface. For clean quartz sand, the Hamaker constant is 8.86×10^{-20} J,[S16] whereas for goethite-coated sand, 5.0×10^{-20} J is utilized;[S17-S19] and A_{33} is the Hamaker constant of water, which is 3.70×10^{-20} J.[S20]

With the assumption of constant potential at the surface, the electrical double layer interaction can be calculated as: [S21]

$$V_{EDL} = \pi r_{NP}\varepsilon_0\varepsilon_r\left\{2\phi_1\phi_2\ln\left[\frac{1+\exp(-\kappa h)}{1-\exp(-\kappa h)}\right] + (\phi_1^2+\phi_2^2)\ln\left[1-\exp(-2\kappa h)\right]\right\} \quad \text{(S5)}$$

where ε_0 is the vacuum permittivity (8.85×10^{-12} C^2/Jm), ε_r is the relative dielectric permittivity of water (78.4), ϕ_1 and ϕ_2 are the surface potentials of GO nanoparticles and sand grains, respectively, κ is the Debye reciprocal length and can be calculated as:[S22]

$$\kappa = \sqrt{\frac{e^2 \sum n_{j0} z_j^2}{\varepsilon_r \varepsilon_0 K_B T}} \quad \text{(S6)}$$

where e is the electron charge (-1.60×10^{-19} C), z_j is the ion valence, n_{j0} is the number concentration of ions in the bulk solution, K_B is Boltzmann constant (1.38×10^{23} J/K), and T is Kelvin temperature (298 K).

The Born repulsive interaction can be calculated as: [S23]

$$V_{BR} = -\frac{A d_0^6}{48 \pi d^8} \quad \text{(S7)}$$

where d_0 is minimum separation distance between the GO and collector (0.158 nm). [S24, S25]

The hydration repulsive interaction can be calculated as: [S23]

$$V_{HR} = E_0 e^{-\frac{d}{\lambda_0}} \quad \text{(S8)}$$

where E_0 is the maximum repulsive energy per unit area at the closet possible separation distance (0.21 J m^{-2}); [S26] λ_0 is a characteristic decay length (0.0635 nm). [S12]

Total interaction energy of the GO–quartz sand (or GO–goethite-coated sand) system at the desired solution chemistry was calculated as follows: [S8]

$$\begin{aligned} V_{TOT} &= V^{VDW}_{EFGH-ABCD}(d) + V^{EDL}_{EFGH-ABCD}(d) + V^{BR}_{EFGH-ABCD}(d) + V^{HR}_{EFGH-ABCD}(d) \\ &- V^{VDW}_{EFGH-A'B'C'D'}(d+h) - V^{EDL}_{EFGH-A'B'C'D}(d+h) - V^{BR}_{EFGH-A'B'C'D}(d+h) - V^{HR}_{EFGH-A'B'C'D}(d+h) \end{aligned} \quad \text{(S9)}$$

S6. Mathematical modeling

A two-site transport model was used to fit the transport data of GO in the absence or presence of surfactants [S27]. The deposition sites in two-site model are divided into an attachment site and a straining site:

$$\frac{\partial C}{\partial t}+\frac{\rho}{\theta}\frac{\partial S_1}{\partial t}+\frac{\rho}{\theta}\frac{\partial S_2}{\partial t}=D\frac{\partial^2 C}{\partial x^2}-v\frac{\partial C}{\partial x} \quad \text{(S6)}$$

$$\frac{\rho}{\theta}\frac{\partial S_1}{\partial t}=K_{\text{att}}\psi_1 C\ ,\ \psi_1=\frac{S_{\max}-S_1}{S_{\max}} \quad \text{(S7)}$$

$$\frac{\rho}{\theta}\frac{\partial S_2}{\partial t}=K_{\text{str}}\psi_2 C\ ,\quad \psi_2=\left(\frac{d_c+z}{d_c}\right)^{-\beta} \quad \text{(S8)}$$

where ρ (g/cm^3) is the dry bulk density of the packed column; θ (-) is its porosity; D (m^2/d) is hydrodynamic dispersion coefficient (0.676 m^2/d); v (m/d) is the pore-water velocity; C (mg/L) is GO concentration in the aqueous phase; S_1 (mg/kg) and S_2 (mg/kg) are concentrations of GO in the attachment site and the straining site, respectively while K_{att} (h^{-1}) and K_{str} (h^{-1}) are the attachment rate and straining rates, correspondingly; ψ_1 (-) and ψ_2 (-) are the blocking factor and straining factor, individually; $S_{\max}$ (mg/kg) is the maximum retention capacity of GO on the attachment site; d_c (cm) is average diameter of the soil grains; z (cm) is the down gradient distance from the porous medium inlet; and β (-) is a fitting parameter that controls the shape of nanoparticle spatial distribution. A value of 0.432 was assigned for β. [S28] The breakthrough curves of GO were fitted with Equations 6–8 using the HYDRUS-1D software, with K_{att}, $S_{\max}$, and K_{str} as the fitting parameters.

Table S1. Mass balance of GO expressed as percentage of effluent Mass, eluted mass during each flushing step, mass recovered from column, and mass retained in column.

Column No.	Porous media	Electrolyte solution	Saponin concentration	pH	Effluent Mass (%)	Eluted mass (%)	mass retained in column [a] (%)	Mass recovered from column (%)	Mass balance [b] (%)
1	sand	10 mM NaCl	/	7.0	43.8 ± 0.3	4.6 ± 0.2	49.6 ± 0.5	51.1 ± 0.2	99.5 ± 0.2
2	goethite-coated sand	10 mM NaCl	/	7.0	1.2 ± 0.1	1.4 ± 0.1	97.6 ± 0.3	95.7 ± 1.5	98.2 ± 0.7
3	sand	10 mM NaCl	3 mg/L	7.0	47.1 ± 1.2	5.4 ± 0.3	47.5 ± 0.6	46.2 ± 0.7	98.7 ± 0.5
4	sand	10 mM NaCl	5 mg/L	7.0	50.2 ± 1.3	5.8 ± 0.2	43.9 ± 1.1	41.4 ± 0.5	97.5 ± 1.1
5	sand	10 mM NaCl	10 mg/L	7.0	54.5 ± 1.0	7.5 ± 0.5	38.0 ± 0.7	35.7 ± 0.3	97.7 ± 0.6
9	goethite-coated sand	10 mM NaCl	3 mg/L	7.0	2.8 ± 0.2	0.9 ± 0.1	96.3 ± 0.5	93.3 ± 0.7	97.0 ± 0.5
7	goethite-coated sand	10 mM NaCl	5 mg/L	7.0	7.5 ± 0.3	1.3 ± 0.1	91.2 ± 0.6	89.2 ± 1.5	97.9 ± 0.3
8	goethite-coated sand	10 mM NaCl	10 mg/L	7.0	14.2 ± 0.3	2.5 ± 0.2	83.3 ± 0.7	79.5 ± 1.2	96.2 ± 0.1
9 [c]	sand	10 mM NaCl	10 mg/L saponin-saturated column	7.0	46.5 ± 1.7	6.0 ± 0.3	47.5 ± 1.1	47.2 ± 0.8	99.7 ± 0.3
10 [c]	goethite-coated sand	10 mM NaCl	10 mg/L saponin-saturated column	7.0	3.4 ± 0.1	0.9 ± 0.1	95.7 ± 1.5	94.0 ± 0.5	98.3 ± 0.1
11	sand	0.1 mM $CuCl_2$	/	5.0	56.0 ± 2.2	5.8 ± 0.5	38.2 ± 0.3	33.8 ± 0.1	95.6 ± 1.3
12	sand	0.1 mM $CuCl_2$	10 mg/L	5.0	63.2 ± 1.7	6.5 ± 0.2	30.3 ± 0.2	26.4 ± 0.3	96.1 ± 1.2
13	goethite-coated sand	0.1 mM $CuCl_2$	/	5.0	2.7 ± 0.7	4.4 ± 0.1	82.5 ± 0.7	81.4 ± 0.5	98.9 ± 1.5
14	goethite-coated sand	0.1 mM $CuCl_2$	10 mg/L	5.0	13.1 ± 1.0	4.6 ± 0.2	66.7 ± 0.5	64.0 ± 0.4	97.3 ± 0.8

[a] Mass retained in column = 100 – effluent mass –eluted mass.

[b] Mass balance was calculated as: (effluent mass + eluted mass + mass recovered from column)/mass injected.

[c] Column was pre-saturated with 10 mg/L saponin before injecting GO suspension.

Table S2. Adsorption capacities of saponin onto porous media under different solution chemistry conditions. Error bars represent standard deviations from replicate experiments (n=3)

No.	Porous media	background solution	Saponin concentration	pH	q (mg/kg)
1	sand	10 mM NaCl	3 mg/L	7.0	11.5 ± 0.2
2	sand	10 mM NaCl	5 mg/L	7.0	17.5 ± 0.2
3	sand	10 mM NaCl	10 mg/L	7.0	32.2 ± 0.1
4	goethite-coated sand	10 mM NaCl	3 mg/L	7.0	12.9 ± 0.1
5	goethite-coated sand	10 mM NaCl	5 mg/L	7.0	20.7 ± 0.3
6	goethite-coated sand	10 mM NaCl	10 mg/L	7.0	38.9 ± 0.5
7	sand	0.1 mM $CuCl_2$	10 mg/L	5.0	38.8 ± 2.0
8	goethite-coated sand	0.1 mM $CuCl_2$	10 mg/L	5.0	41.9 ± 0.1

Table S3. The sizes of GO under different solution chemistry conditions

No.	Electrolyte solution	Saponin concentration	pH	the sizes of GO [a]
1	10 mM NaCl	/	7.0	535.2 ± 35.7
2	10 mM NaCl	3 mg/L	7.0	478.7 ± 26.9
3	10 mM NaCl	5 mg/L	7.0	415.5 ± 22.3
4	10 mM NaCl	10 mg/L	7.0	349.1 ± 12.8
5	0.1 mM $CuCl_2$	/	5.0	565.6 ± 27.9
6	0.1 mM $CuCl_2$	10 mg/L	5.0	437.8 ± 21.5

[a] The average diameter of GO which was determined by measuring 120 GO nanosheets in multi-TEM images (Fig. S9) using Nano Measurer 1.2.5 software.

Table S4. Calculated maximum energy barriers (Φ_{max}), secondary energy minimum depth (Φ_{sec}), and the respective separation distances of particle–collector XDLVO interaction energy profiles.

Column No.	Porous media	Electrolyte solution	Saponin concentration	pH 7.0	Φ_{max}		Φ_{sec}	
					height (K_BT)	distance (nm)	depth (K_BT)	distance (nm)
1	sand	10 mM NaCl	/	7.0	704.9	4.0	-26.4	19
2	goethite-coated sand	10 mM NaCl	/	7.0	50.1	5.8	-35.3	22
3	sand	10 mM NaCl	3 mg/L	7.0	1503.2	3.5	-9.6	24
4	sand	10 mM NaCl	5 mg/L	7.0	2695.8	2.7	-7.7	26
5	sand	10 mM NaCl	10 mg/L	7.0	3370.3	2.0	-6.5	24
6	goethite-coated sand	10 mM NaCl	3 mg/L	7.0	650.0	4.2	-11.0	22
7	goethite-coated sand	10 mM NaCl	5 mg/L	7.0	1397.1	2.8	-7.6	22
8	goethite-coated sand	10 mM NaCl	10 mg/L	7.0	2175.5	2.5	-6.1	18
11	sand	0.1 mM $CuCl_2$	/	5.0	1350.2	2.0	-53.3	16
12	sand	0.1 mM $CuCl_2$	10 mg/L	5.0	2133.5	1.8	-12.5	17
13	goethite-coated sand	0.1 mM $CuCl_2$	/	5.0	545.2	1.9	-45.7	15
14	goethite-coated sand	0.1 mM $CuCl_2$	10 mg/L	5.0	1387.6	1.7	-10.5	12

Table S5. Fitted parameters of two-site transport model from breakthrough results of column experiments.

Column No.	Porous media	Electrolyte solution	Saponin concentration	pH 7.0	Parameters of two-site transport model			
					K_{att} (h^{-1})	S_{max} (mg/kg)	K_{str} (h^{-1})	R^2
1	sand	10 mM NaCl	/	7.0	4.812	0.612	1.335	0.989
2	goethite-coated sand	10 mM NaCl	/	7.0	28.85	2.519	17.83	0.961
3	sand	10 mM NaCl	3 mg/L	7.0	3.697	0.418	0.976	0.983
4	sand	10 mM NaCl	5 mg/L	7.0	1.682	0.368	0.682	0.979
5	sand	10 mM NaCl	10 mg/L	7.0	0.535	0.209	0.181	0.977
6	goethite-coated sand	10 mM NaCl	3 mg/L	7.0	17.67	1.580	13.02	0.960
7	goethite-coated sand	10 mM NaCl	5 mg/L	7.0	12.96	0.981	8.591	0.952
8	goethite-coated sand	10 mM NaCl	10 mg/L	7.0	5.979	0.429	5.15	0.966
9 [a]	sand	10 mM NaCl	10 mg/L saponin-saturated column	7.0	3.120	0.457	1.02	0.965
10 [a]	goethite-coated sand	10 mM NaCl	10 mg/L saponin-saturated column	7.0	15.82	0.653	12.73	0.955
11	sand	0.1 mM $CuCl_2$	/	5.0	0.789	0.144	0.894	0.955
12	sand	0.1 mM $CuCl_2$	10 mg/L	5.0	0.289	0.296	0.117	0.963
13	goethite-coated sand	0.1 mM $CuCl_2$	/	5.0	25.29	0.696	7.756	0.963
14	goethite-coated sand	0.1 mM $CuCl_2$	10 mg/L	5.0	4.129	0.569	2.257	0.979

[a] Column was pre-saturated with 10 mg/L saponin before injecting GO suspension.

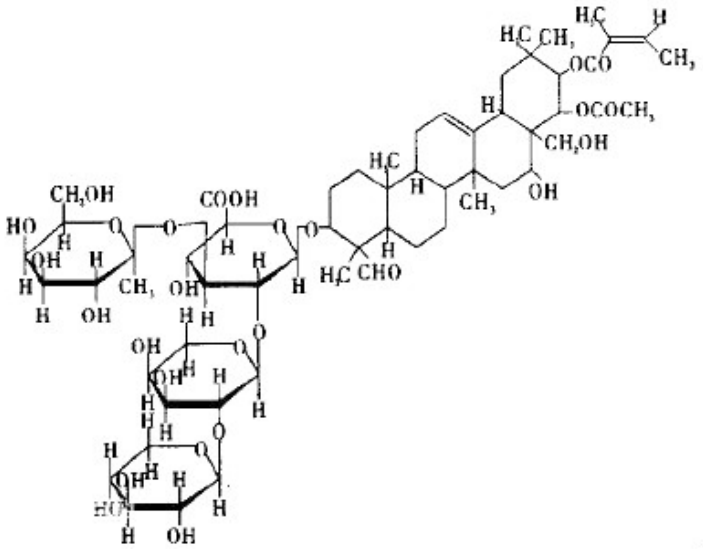

Fig. S1. Chemical structure of saponin.[S28] The molecular sizes of saponin (25.9 Å × 13.2 Å × 19.1 Å) was obtained from molecular simulation using Chemoffice 2004 and GaussView 5.0.

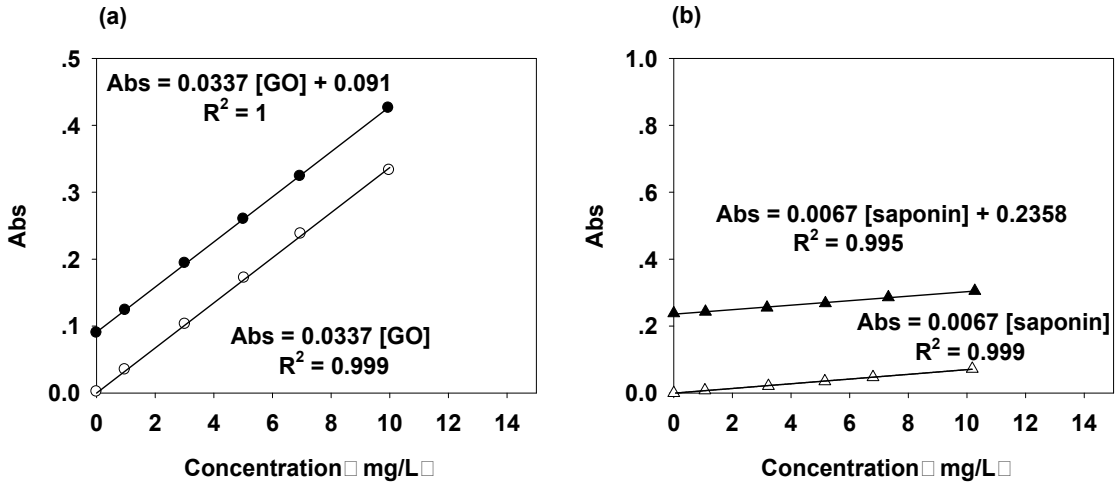

Fig. S2. Calibration curves of GO and saponin used to calculate the concentrations of GO in the presence of saponin and vice versa (Chen et al., 2012). Left panels show the UV absorbance of GO (at 230 nm) as a function of GO concentration in the absence of saponin (hollow symbols ○), and in the presence of 10 mg/L saponin (filled symbols ●). Right panels show the absorbance of saponin (at 263 nm) as a function of saponin concentration in the absence of GO (hollow symbols Δ), and in the presence of 10 mg/L GO (filled symbols ▲).

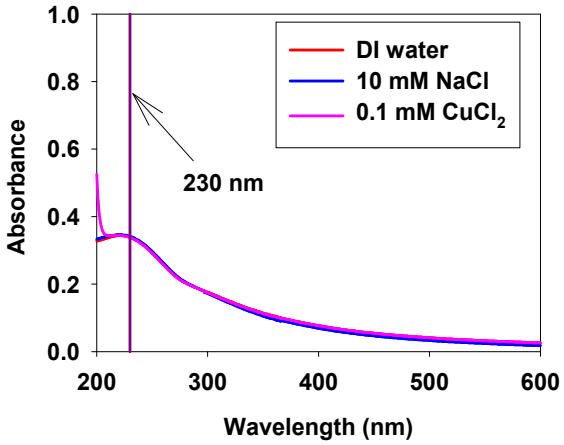

Fig. S3. Effects of aggregation of GO on UV absorbance of GO at 230 nm.

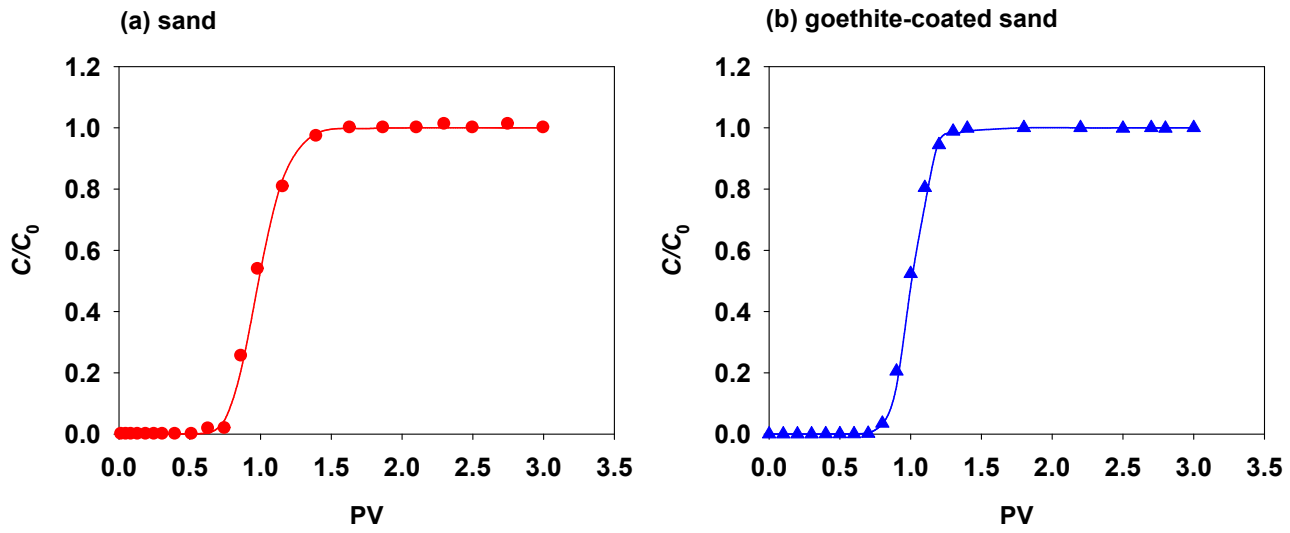

Fig. S4. Representative breakthrough curve of conservative tracer (Br^-) in (a) quartz sand and (b) goethite-coated sand. The line was plotted by fitting the breakthrough data with the one-dimensional steady-state advection-dispersion equation**.**

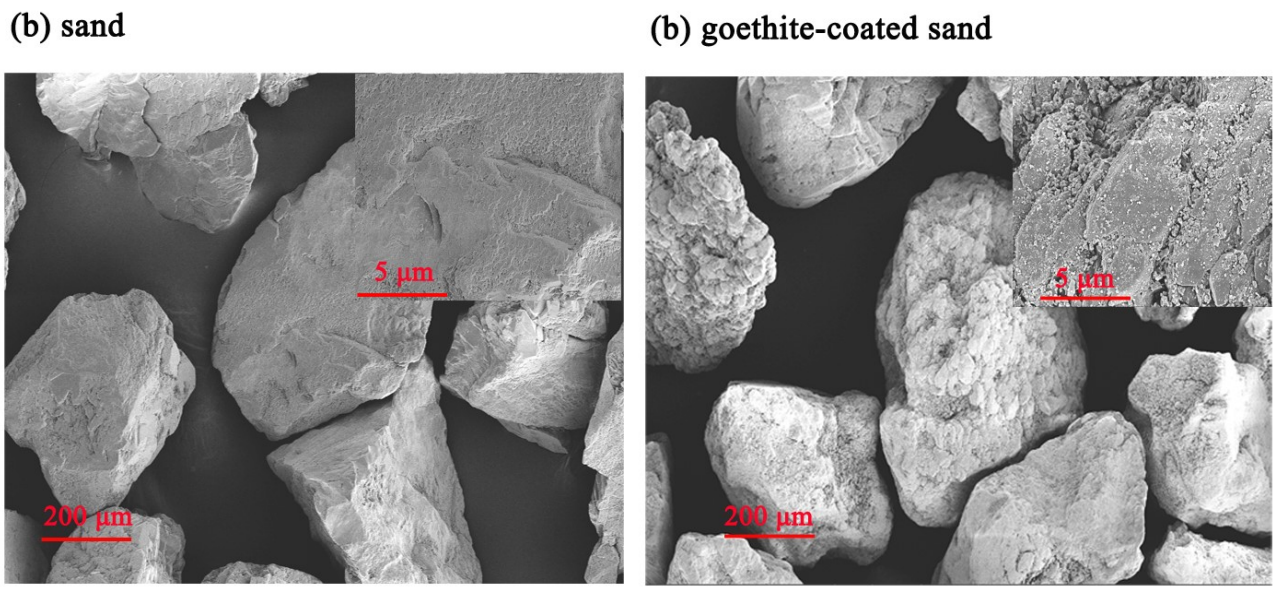

Fig. S5. Scanning electron microscope (SEM) images of (a) quartz sand and (b) goethite-coated sand. The inset of images show characteristic micro-structures of porous media.

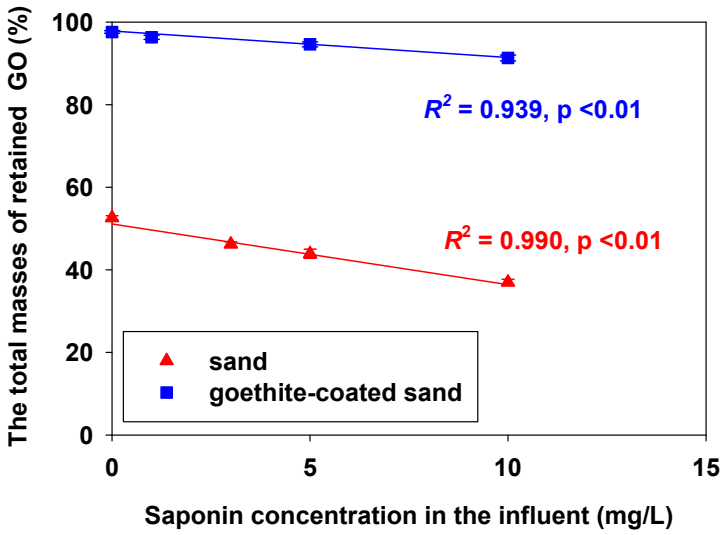

Fig. S6. Comparison between the total masses of retained GO in the columns and concentrations of saponin in the influent for columns 1–8.

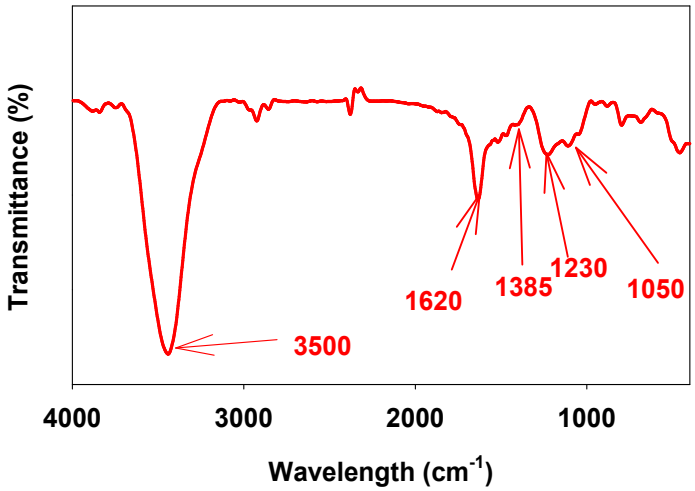

Fig. S7. (a) Fourier transform infrared (FTIR) transmission spectra of graphene oxide (GO). The following features are observed:[S29] 3500 cm^{-1} (O-H stretching vibrations), 1620 cm^{-1} (C=C stretching, skeletal vibrations from unoxidized graphitic domains), 1385 cm^{-1} (O-H bending vibrations from hydroxyl groups), 1230 cm^{-1} (breathing vibrations from epoxy groups), and 1050 cm^{-1} (C-O stretching vibrations).

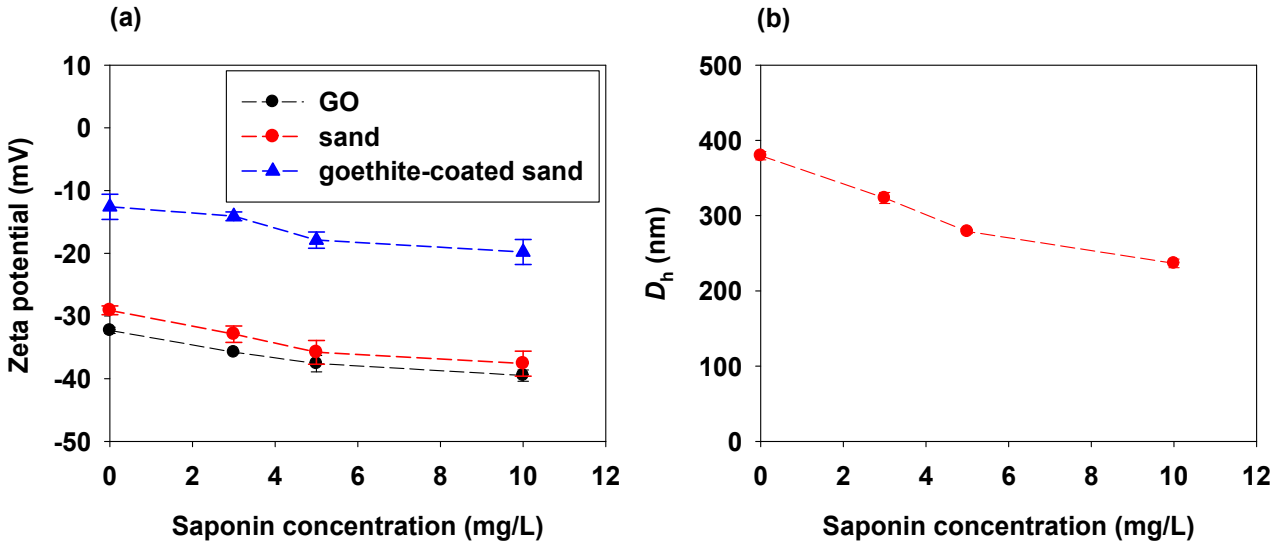

Fig. S8. (a) ζ-potential of GO, sand, and goethite-coated sand as affected by saponin at 10 mM NaCl; (b) hydrodynamic diameter (Z_{avg}) of GO as affected by saponin at 10 mM NaCl.

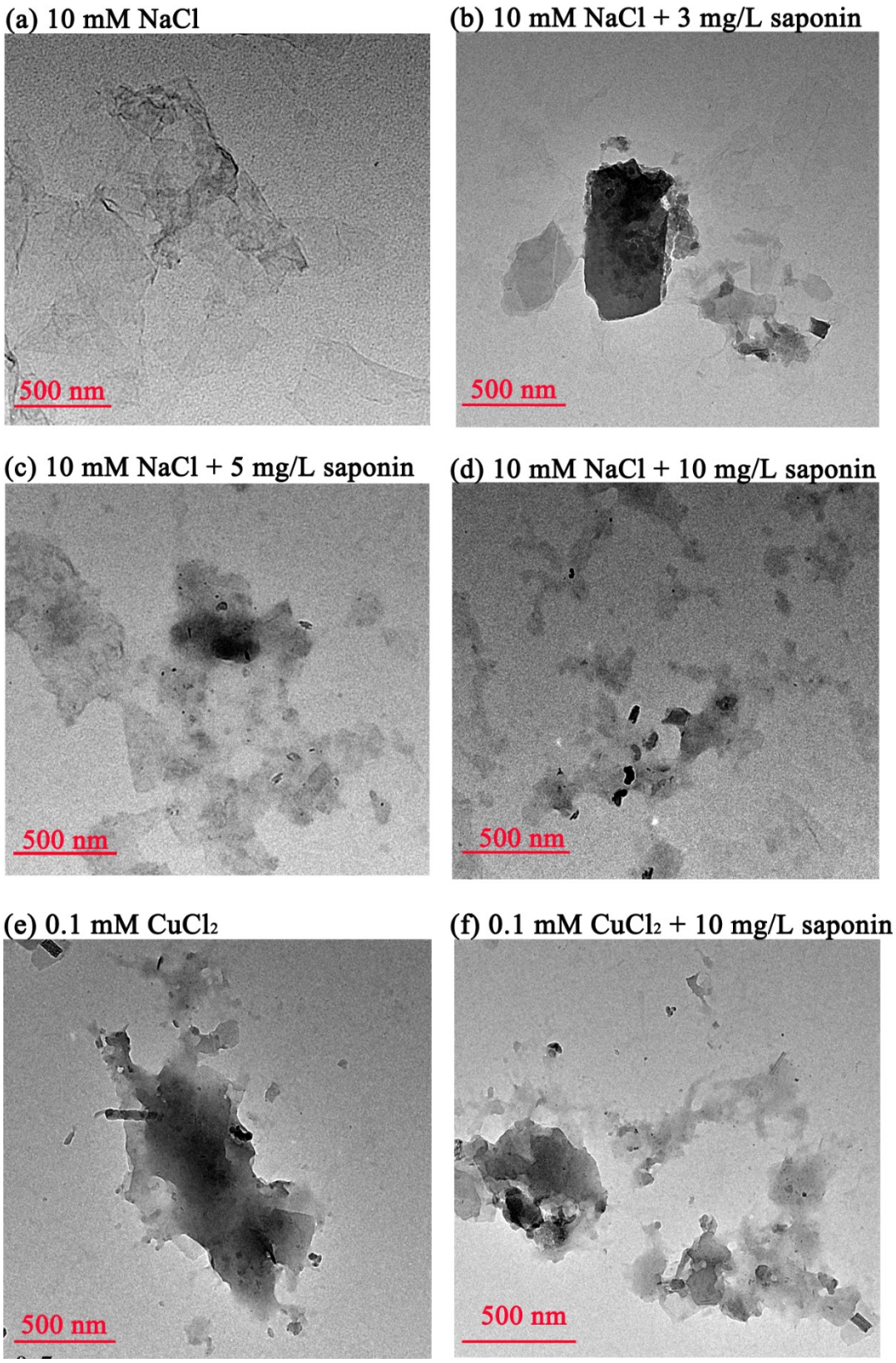

Fig. S9. Representative TEM images of GO (~10 mg/L) under different solution chemistry conditions.

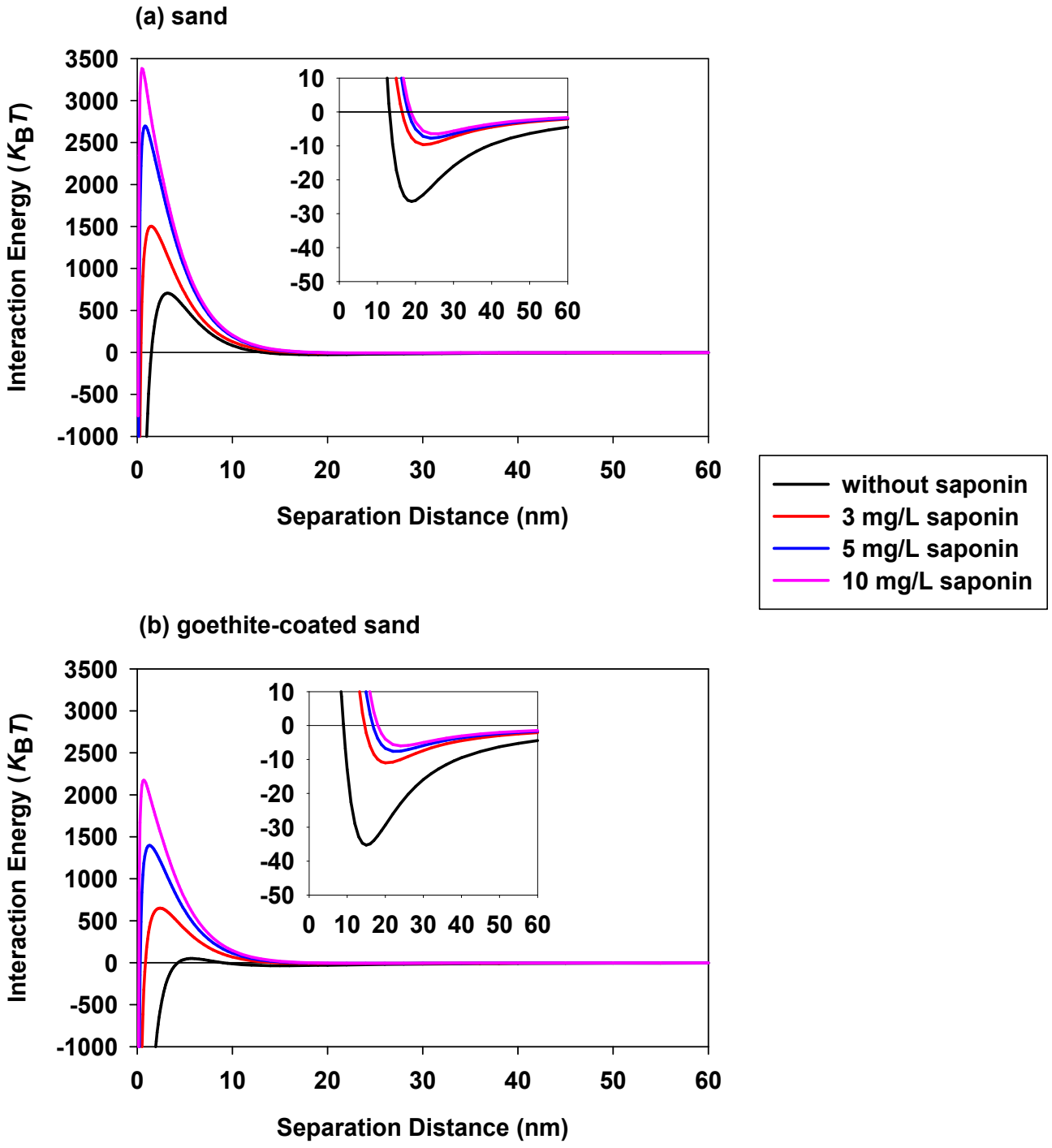

Fig. S10. Effect of saponin on the XDLVO particle–collector interaction energy profiles (Na^+ was the background cation): (a) GO and sand; (b) GO and goethite-coated sand. The insets are plotted on a smaller y-axis scale to highlight the secondary minimum depth.

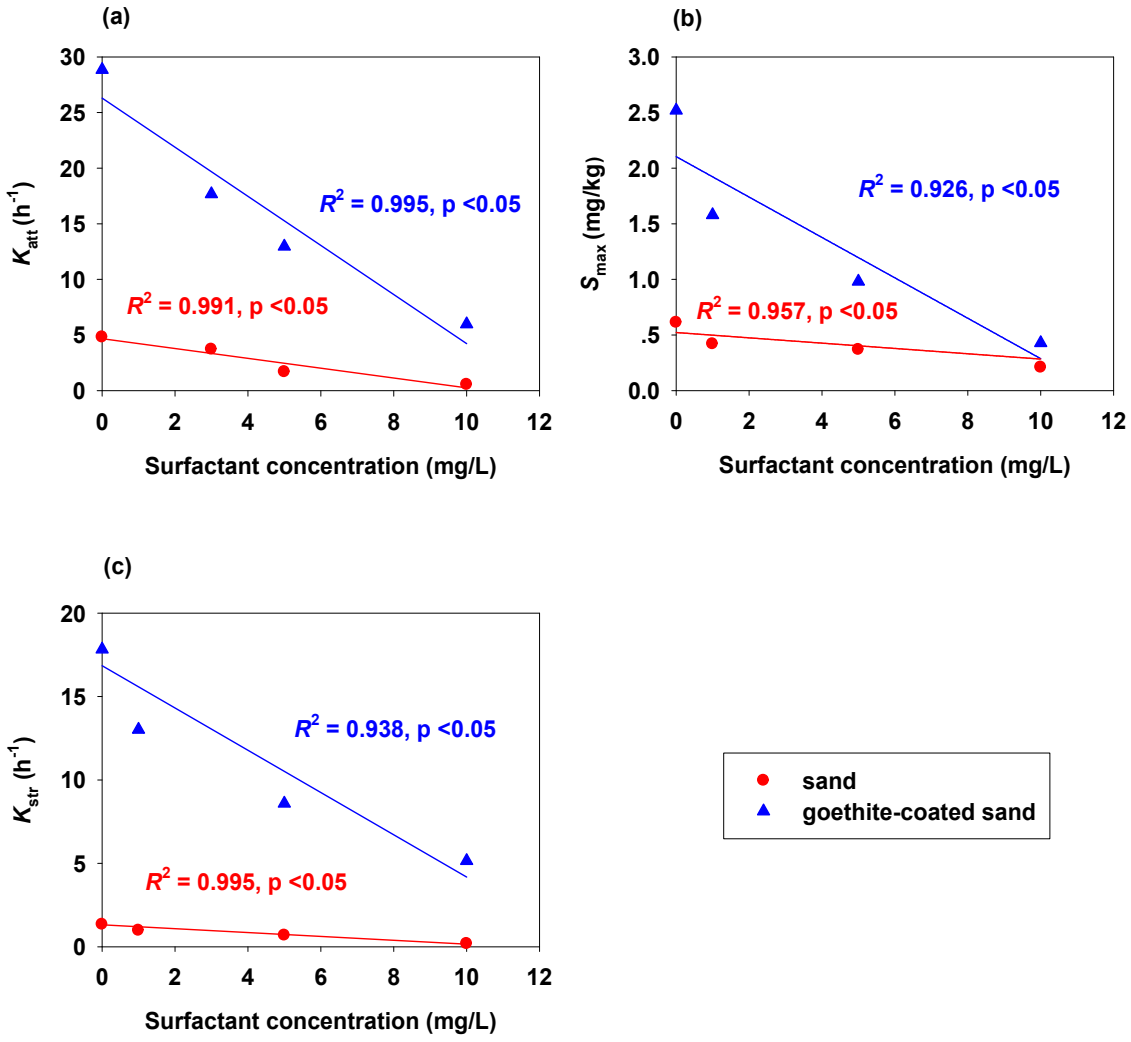

Fig. S11. Correlations between fitted parameters of two-site transport model (based on breakthrough data of columns 1–8) and saponin concentration.

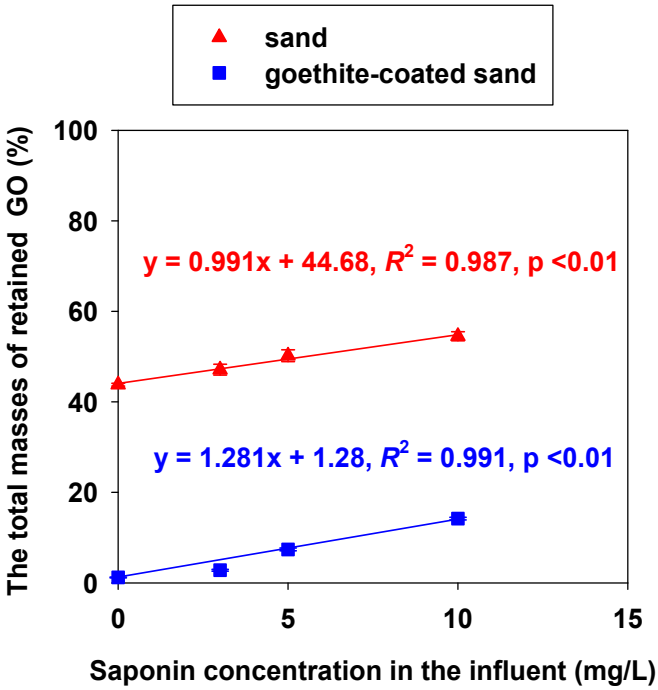

Fig. S12. (a) Comparison between the total masses of retained GO in the columns and concentrations of saponin in the influent for columns 1–8. The total mass of retained GO in column = ((influent mass – effluent mass)/influent mass) ×100%.

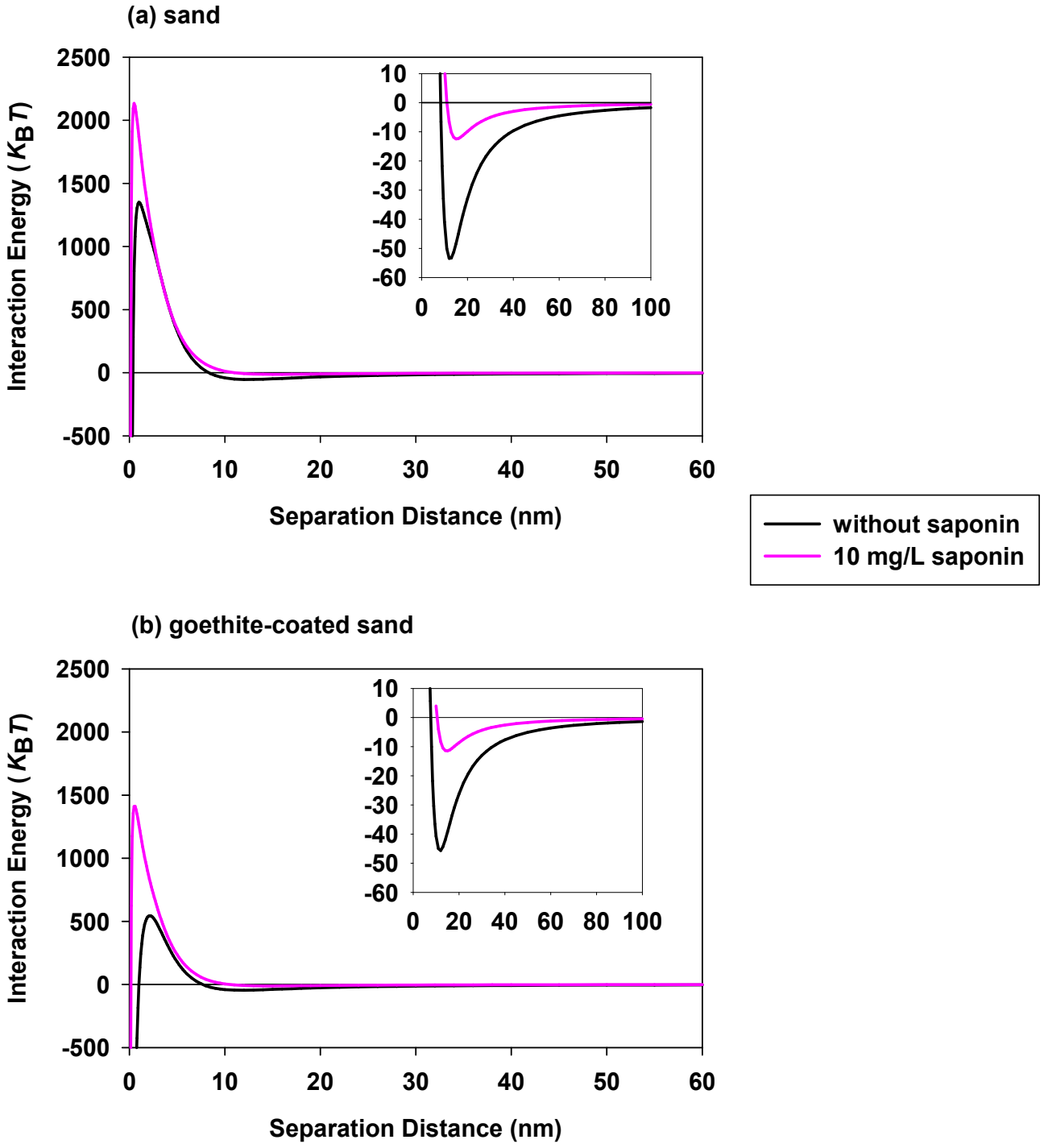

Fig. S13. Effect of saponin on the XDLVO particle-collector interaction energy profiles (Cu^{2+} was the background cation): (a) GO and sand; (b) GO and goethite-coated sand. The insets are plotted on a smaller y-axis scale to highlight the secondary minimum depth.

References:

S1. T. Xia, Y. Lin, X. Guo, S. Li, J. Cui, H. Ping, J. Zhang, R. Zhong, L. Du, C. Han and L. Zhu, Co-transport of graphene oxide and titanium dioxide nanoparticles in saturated quartz sand: Influences of solution pH and metal ions, *Environ. Pollut.*, 2019, **51,** 723–730.

S2. R.S. Stahl and B.R. James, Zinc sorption by iron-oxide-coated sand as a function of pH, *Soil Sci. Soc. Am. J.*, 1991, **55,** 1291–1294.

S3. P.N. Mitropoulou, V.I. Syngouna and C.V. Chrysikopoulos, Transport of colloids in unsaturated packed columns: Role of ionic strength and sand grain size, Chem. Eng. J., 2013, 232, 237–248.

S4. C.V. Chrysikopoulos, N.P. Sotirelis and N.G. Kallithrakas-Kontos, Cotransport of graphene oxide nanoparticles and kaolinite colloids in porous media, *Transport Porous Med.*, 2017, **219,** 1−24.

S5. Z. Qi, L. Zhang, F. Wang, L. Hou and W. Chen, Factors controlling transport of graphene oxide nanoparticles in saturated sand columns, *Environ. Toxicol. Chem.*, 2014, **33,** 998–1004.

S6. G. Chen, X. Liu and C. Su, Distinct effects of humic acid on transport and retention of TiO2 rutile nanoparticles in saturated sand columns, *Environ. Sci. Technol.*, 2012, 46, 7142–7150.

S7. S. Song, L. Zhu and W. Zhou, Simultaneous removal of phenanthrene and cadmium from contaminated soils by saponin, a plant-derived biosurfactant, *Environ. Pollut.*, 2008, **15,** 1368–1370.

S8. D. Wang, C. Shen, Y. Jin, C. Su, L. Chu and D. Zhou, Role of solution chemistry in the retention and release of graphene oxide nanomaterials in uncoated and iron oxide-coated sand, *Sci. Total Environ.*, 2017, **579,** 776–785.

S9. Z. Qi, L. Hou, D. Zhu, R. Ji and W. Chen, Enhanced transport of phenanthrene and 1-naphthol by colloidal graphene oxide nanoparticles in saturated soil, *Environ. Sci. Technol.*, 2014, **48,** 10136–10144.

S10. Z. Qi, L. Zhang and W. Chen, Transport of graphene oxide nanoparticles in saturated sandy soil, *Environ. Sci. Proc. Impacts*, 2014, **16,** 2268–2277.

S11. Z. Qi, L. Zhang, F. Wang, L. Hou and W. Chen, Factors controlling transport of graphene oxide nanoparticles in saturated sand columns, *Environ. Toxicol. Chem.*, 2014, **33,** 998–1004.

S12. E. Pazmino, J. Trauscht, B. Dame and W.P. Johnson, Power law size-distributed heterogeneity explains colloid retention on soda lime glass in the presence of energy barriers, *Langmuir*, 2014, **30,** 5412–5421.

S13. J. Gregory, Approximate expressions for retarded van der waals interaction, *J. Colloid Interf. Sci.*, 1981, **83,**138–145.

S14. J. Bergendahl and D.Grasso, Prediction of colloid detachment in a model porous media: *Thermodynamics, Aiche J.*, 1999, **45,** 475–484.

S15. L. Feriancikova and S. Xu, Deposition and remobilization of graphene oxide within saturated sand packs, *J. Hazard. Mater.*, 2012, **235–236,** 194–200.

S16. L. Bergstrom, Hamaker constants of inorganic materials, *Adv. Colloid Interface Sci.*, 1997, **70,** 125–169.

S17. B. Faure, G. Salazar-Alvarez and L. Bergstrom, Hamaker constants of iron oxide nanoparticles, *Langmuir*, 2011, **27,** 8659–8664.

S18. D. Wang, W. Zhang and D. Zhou, Antagonistic effects of humic acid and iron oxyhydroxide grain-coating on biochar nanoparticle transport in saturated sand, *Environ. Sci. Technol.*, 2013, **47,** 5154–5161.

S19. D. Wang, Y. Jin and D. P. Jaisi, Effect of size-selective retention on the cotransport of hydroxyapatite and goethite nanoparticles in saturated porous media, *Environ. Sci. Technol.*, 2015, **49,** 8461–8470.

S20. J. N. Israelachvili, Intermolecular and surface forces, Academic Press: San Diego, CA. 1992.

S21. M. Elimelech and C.R. O'Melia, Effect of particle size on collision efficiency in thedeposition of Brownian particles with electrostatic energy barriers, Langmuir, 1990, **6,** 1153–1163.

S22. W. B. Russel, D. A. Saville and W. R. Schowalter, Colloidal Dispersions. Cambridge University Press, Cambridge. 1989.

S23. R. Oliveira Understanding adhesion: A means for preventing fouling, *Exp. Therm. Fluid Sci.*, 1997, **14,** 316–322.

S24. E.M.V. Hoek and G.K. Agarwal, Extended DLVO interactions between spherical particles and rough surfaces, *J. Colloid Interface Sci.*, 2006, **298,** 50–58.

S25. C.J. van Oss, Interfacial Forces in Aqueous Media. CRC Press, Taylor & Francis 1994, Marcel Dekker Inc., New York, NY.

S26. E.M.V. Hoek, S. Bhattacharjee and M. Elimelech, Effect of membrane surface roughness on colloid-membrane DLVO interactions, *Langmuir*, 2003, **19,** 4836–4847.

S27. S. A. Bradford, J. Simunek, M. Bettahar, M.T. Van Genuchten and S.R. Yates, Modeling colloid attachment, straining, and exclusion in saturated porous media, *Environ. Sci. Technol.*, 2003, **37,** 2242–2250.

S28. C.N. Mulligan, Recent advances in the environmental applications of biosurfactants, Curr. Opin. *Colloid Interf. Sci.*, 2009, 1**4,** 372–378.

S29. M. Wang, Y. Song, H. Zhang, T. Lu, W. Chen, W. Li, W. Qi and Z. Qi, Insights into the mutual promotion effect of graphene oxide nanoparticles and tetracycline on their transport in saturated porous media, *Environ. Pollut.*, 2021, **268,** 115730.